Journal of Innate Immunity

Research Article

J Innate Immun 2021;13:225–241
DOI: 10.1159/000514885

Received: December 8, 2020
Accepted: January 22, 2021
Published online: April 15, 2021

Interleukin 8 Elicits Rapid Physiological Changes in Neutrophils That Are Altered by Inflammatory Conditions

Stefan Bernhard[a] Stefan Hug[a] Alexander Elias Paul Stratmann[a] Maike Erber[a] Laura Vidoni[a] Christiane Leonie Knapp[a] Bertram Dietrich Thomaß[a] Michael Fauler[b] Bo Nilsson[c] Kristina Nilsson Ekdahl[c, d] Karl Föhr[e] Christian Karl Braun[a, f] Lisa Wohlgemuth[a] Markus Huber-Lang[a] David Alexander Christian Messerer[a, e]

[a]Institute of Clinical and Experimental Trauma Immunology, University Hospital of Ulm, Ulm, Germany; [b]Institute of General Physiology, University of Ulm, Ulm, Germany; [c]Rudbeck Laboratory, Department of Immunology, Genetics and Pathology, Uppsala University, Uppsala, Sweden; [d]Centre of Biomaterials Chemistry, Linnaeus University, Kalmar, Sweden; [e]Department of Anesthesiology and Intensive Care Medicine, University Hospital of Ulm, Ulm, Germany; [f]Department of Pediatrics and Adolescent Medicine, University Hospital of Ulm, Ulm, Germany

Keywords
Neutrophil granulocytes · Intracellular pH · Lipopolysaccharide · Sodium-proton exchanger 1 · Flow cytometry; Interleukin 8

Abstract
A sufficient response of neutrophil granulocytes stimulated by interleukin (IL)-8 is vital during systemic inflammation, for example, in sepsis or severe trauma. Moreover, IL-8 is clinically used as biomarker of inflammatory processes. However, the effects of IL-8 on cellular key regulators of neutrophil properties such as the intracellular pH (pH_i) in dependence of ion transport proteins and during inflammation remain to be elucidated. Therefore, we investigated in detail the fundamental changes in pH_i, cellular shape, and chemotactic activity elicited by IL-8. Using flow cytometric methods, we determined that the IL-8-induced cellular activity was largely dependent on specific ion channels and transporters, such as the sodium-proton exchanger 1 (NHE1) and non-NHE1-dependent sodium flux. Exposing neutrophils in vitro to a proinflammatory micromilieu with N-formyl-Met-Leu-Phe, LPS, or IL-8 resulted in a diminished response regarding the increase in cellular size and pH. The detailed kinetics of the reduced reactivity of the neutrophil granulocytes could be illustrated in a near-real-time flow cytometric measurement. Last, the LPS-mediated impairment of the IL-8-induced response in neutrophils was confirmed in a translational, animal-free human whole blood model. Overall, we provide novel mechanistic insights for the interaction of IL-8 with neutrophil granulocytes and report in detail about its alteration during systemic inflammation.

Introduction

Neutrophil granulocytes are the most abundant cells of the innate immune system. An appropriate activation of these cells is vital for the sufficient clearance of pathogens, particularly during systemic inflammation as in

karger@karger.com
www.karger.com/jin

Correspondence to:
David Alexander Christian Messerer, david.messerer@uni-ulm.de

sepsis. Following stimulation with potent chemoattractants, including the complement activation product 5a (C5a) and the chemokine interleukin (IL)-8 (synonym: C-X-C motif chemokine ligand 8, CXCL8), neutrophils become activated and migrate to the inflammatory environment, where they form the "first cellular line of defense" [1–3]. However, prolonged and excessive inflammatory stimulation can lead to neutrophil dysregulation and dysfunction, which represent major drivers of innate immune dysfunction and multiorgan dysfunction syndrome during sepsis [4, 5].

ILs such as IL-6 and IL-8 are widely used as a diagnostic and prognostic marker for infectious (e.g., septic) and other inflammatory (e.g., traumatic) conditions [6, 7]. However, the relevance of IL-8 during systemic inflammation is not completely understood [6–9]. The main function of IL-8 regarding neutrophils is the induction of chemotaxis. In addition, IL-8 causes a release of lysosomal enzymes, an upregulation of adhesion molecules, an increase of intracellular calcium, and priming of the oxidative burst [10–14]. These effector functions are mediated by two G-protein coupled chemokine receptors CXCR1 (CD181) and CXCR2 (CD182), with CXCR2 being more relevant for chemotaxis and cellular functions during inflammatory conditions and being significantly downregulated in patients with sepsis [15–17].

Exposure of neutrophils to chemoattractants, for example, C5a or N-formyl-Met-Leu-Phe (fMLF, formerly termed fMLP), resulted in a defined cellular response as reported in previous studies. This process involves a rise in intracellular calcium, cellular depolarization, and intracellular alkalization as well as a change in cellular morphology toward an oval shape, and activation of glucose uptake (GlcU) [18–23]. There is increasing evidence that these cellular responses after stimulation become defective in the setting of systemic inflammation [19–22] and thus are hallmarks of neutrophil dysfunction under such conditions. Consequently, they are of growing interest as diagnostic and/or prognostic markers and promote the development of immunomodulatory strategies during excessive inflammation [22–24]. Moreover, the relevance of these physiological parameters is illustrated by the fact that they are closely associated with cellular effector functions. For example, a lower cytosolic pH is associated with higher rates of apoptosis and a reduced ability to migrate, whereas an alkaline pH seems to prevents apoptosis [25, 26]. In addition, changes in intracellular pH (pH_i) modulate cellular migration of neutrophils [27–30].

A previous report demonstrated that after IL-8 stimulation, similar cellular changes may occur in adherent neutrophils, including transient depolarization and alkalization [29]. However, the mechanistic involvement of various ion transport proteins in these alterations and the relationship with an inflammatory environment are hitherto not completely elucidated [29, 31, 32]. Several studies indicated the relevance of these underlying ion currents and signaling mechanisms, both for the regulation of cellular effector functions and inflammatory processes [20, 21, 24, 28, 30, 33]. Of note, these studies were frequently performed with adherent cells and/or in the absence of extracellular HCO_3^- in the buffer medium, although this ion is essential for physiological homeostasis and is involved in transport processes that are relevant for various neutrophil functions [20, 34–36]. Furthermore, IL-8 has been linked to changes in crucial immune functions, for example, chemotaxis and NETosis [14, 37], rendering a change in pH_i and metabolism likely. In this context, antagonists of IL-8 are already used in the treatment of severe inflammatory conditions. However, the data are still limited and partly inconsistent [38–40]. Overall, IL-8 clearly plays an important role during systemic inflammation [6, 9, 10, 41, 42]. Therefore, a better understanding of the IL-8-induced neutrophil activation and particularly its underlying mechanisms during systemic inflammation are of great scientific and clinical interest because they might reveal pharmacological targets for the regulation of an IL-8-induced excessive inflammatory response and to identify potential diagnostic markers of cellular dysfunction in sepsis.

In the present study, we (1) analyze the rapid physiological response of neutrophils upon IL-8 stimulation, (2) compare it with the response to other clinically relevant inflammatory mediators, (3) identify involved ion channels and transporters, and (4) report significant changes of IL-8-induced responses during ex vivo simulated sepsis.

Materials and Methods

All reagents were purchased from Merck (Darmstadt, Germany), when not indicated otherwise.

Granulocyte Preparation

Following ethical approval by the Local Independent Ethics Committee of the University of Ulm (number 459/18; 94/14), informed written consent was obtained from healthy human volunteers (age 18–35 years, male and female) without acute or chronic medication and with no signs of infection. Whole blood was drawn by peripheral venipuncture as described by the World Health Or-

ganization guidelines [43]. Blood was drawn into syringes containing 3.2% trisodium citrate (Sarstedt, Nümbrecht, Germany). Neutrophils were isolated by Ficoll-Paque (GE Healthcare, Uppsala, Sweden) density gradient centrifugation (30 min, 340 g, room temperature) and subsequent dextran sedimentation (30 min, room temperature). Residual erythrocytes were removed by hypotonic lysis (10 s of resuspension in distilled and sterile water). Hypotonic lysis might affect forward scatter of neutrophils; however, in previous experiments, cellular swelling relapsed to baseline level if isotonicity is restored [44]. For faster preparation of neutrophils in the presence of other leukocytes, the initial density gradient centrifugation was skipped. All experiments were conducted with isolated neutrophils if not indicated otherwise (see online suppl. Table 1; see www.karger.com/doi/10.1159/000514885 for all online suppl. material). The cell count was adjusted to 2×10^6 cells/mL and stored in Hank's Balanced Salt Solution ($HBSS^{+/+}$; Thermo Fisher, Darmstadt, Germany) adjusted to a pH of 7.3 until later use.

Flow Cytometry and Neutrophil Stimulation

Human neutrophils were gated based on their properties of forward and sideward scatter area and analyzed as described previously [19–21] and summarized in online suppl. Figure 1. The forward scatter area (FSC) was assessed as a surrogate for the cellular cell shape (a rise indicating an elongated cellular shape with an increased length/width ratio [20]) and the side scatter area (SSC) for cellular granularity. The fluorescent dyes bis(1,3-dibutylbarbituric acid) trimethine oxonol ($DiBAC_4[3]$), 50 nM, and SNARF™ 5-(and-6)-carboxy-SNARF-1 (SNARF), 1 μM (Thermo Fisher), and 2-deoxy-2-([7-nitro-2,1,3-benzoxadiazol-4-yl]amino)-D-glucose (2NBDG), 30 μM, were used to determine membrane potential (MP), pH_i, and GlcU, respectively. For the FSC, MP, and pH_i, cells were stained for 20 min in $HBSS^{+/+}$ pH 7.3 in a dark water bath at 37°C with the respective dye. Following centrifugation (340 g, 5 min, room temperature), neutrophils were resuspended in RPMI medium with an extracellular pH (pH_e) adjusted to 7.3, when not indicated otherwise. To cells stained with $DiBAC_4[3]$, the dye was added again for 10 min after centrifugation. For the GlcU, cells were resuspended in RPMI and directly stained with 2NBDG. Following a resting period of 10 min, the cells were stimulated with IL-8 (0.05–500; 50 ng/mL (corresponding to 6 nM) when not indicated otherwise), C5a (100 ng/mL = 9.1 nM; Complement Technology, Tyler, TX, USA), fMLF (10 μM), IL-1β (500 pg/mL = 29 pM), IL-6 (2 ng/mL = 90 pM), IL-10 (500 pg/mL = 29 pM), IL-13 (10 ng/mL = 800 pM), LPS (100 ng/mL), or LPS-binding protein (LBP; 2 ng/mL). For the measurement of near-real-time kinetics, the neutrophils were acquired for a 5-min period continuously and analyzed using the statistic language R (R Core Team, Vienna, Austria). Time-series data were smoothed by applying a nonweighted moving average with a window width of 1 s containing an average of 3,019 ± 498 neutrophils per second. All data were acquired with a FACSCantoII cytometer (BD Biosciences, Heidelberg, Germany). Absolute values of FSC differ in online suppl. Figure 2 since they have been generated after a routine recalibration of the device, however, with little effects to relative changes induced by IL-8.

Coulter Counter

To investigate changes in cell volume and diameter, isolated neutrophils were stimulated for 10 min and measured using a cell counter working through electronic current exclusion (Cell Counter CASY, OLS OMNI Life Science, Bremen, Germany).

Ion Channel Modulators, Extracellular Acidosis, and LPS Preincubation

To determine the involved ion transport proteins and underlying intracellular signaling pathways of the IL-8-induced effects, neutrophils were incubated at 37°C with the subsequently listed substances (their proposed targets are given within the brackets): amiloride (200 μM, 10 min, Na^+-channels), (4-cyanobenzo[b]thiophene-2-carbonyl)guanidine, methanesulfonate (5 μM, 10 min, sodium-proton exchanger 1 [NHE1]; Calbiochem, Darmstadt, Germany), omeprazole (10 μM, 30 min, H^+/K^+-ATPase), NPPB (100 μM, 10 min, Cl^--channels), UK5099 (400 μM, 30 min, mitochondrial pyruvate carrier [MPC]), $ZnCl_2$ (50μM, 30 min, voltage-gated H^+ channel), KB-R7943 (5 μM, 30 min, Na^+/Ca^{2+} exchanger), thapsigargin (2 μM, 30 min, reuptake inhibitor of Ca^{2+} into the endoplasmatic reticulum), W7 (40 μM, 30 min, calmodulin), SKF-96365 (50 μM, 30 min, blocker of the receptor-mediated Ca^{2+} entry from the extracellular medium), DPI (100 μM, 30 min, NADPH oxidase), suramin (200 μM, 30 min, P2Y receptor), 2-deoxyglucose (2 mM, 30 min, glycolysis antimetabolite), $CuSO_4$ (1 mM, 10 min, aquaporin 9), DMOG (1 mM, 30 min, hypoxia inducible factor 1-alpha inductor), calphostin C (50 nM, 30 min, protein kinase C [PKC] inhibitor; Cayman Chemicals, Hamburg, Germany), S0859 (30 μM, 30 min, Na^+/HCO_3^- cotransporter [NBC], monocarboxylate transporter), BAPTA-AM (10 μM, 30 min, chelator of intracellular Ca^{2+}), Y-27623 (10μM, 30 min, rho-kinase inhibitor), nifedipine (3 μM, 5 min, L-type Ca^{2+} channel), and ouabain (100 μM, 30 min, Na^+/K^+-ATPase). After pre-incubation, the samples were split and treated as control or stimulated with IL-8.

Extracellular alkalosis or acidification was achieved by resuspending neutrophils in RPMI adjusted to a pH of 6.6, 7.0, 7.4, or 7.8 with either HCl or NaOH, respectively, followed by an incubation period in the altered medium for 10 min prior to measurement. For the in vitro pretreatment with LPS or chemokines, neutrophils were incubated in $HBSS^{+/+}$ pH 7.3 for 1 h with LPS (100 ng/mL), LPS (100 ng/mL) and LBP (2 ng/mL), fMLF (10 μM), or IL-8 (50 ng/mL). Subsequently, the cells were centrifuged and resuspended in RPMI pH 7.3 as well as the previously supplemented substance.

RNA Extraction and Real-Time PCR

Isolated neutrophils were incubated in $HBSS^{+/+}$ adjusted to a pH of 7.3 with or without LPS 100 + LBP 2 ng/mL for 1 h. After centrifugation for 5 min with 300 g at 4°C, neutrophils were resuspended in TRIzol (Thermo Fisher Scientific, Rockford, IL, USA) in order to isolate RNA according to the manufacturer's protocol. The RNA yield was quantified with a Qubit 2.0 fluorometer using the Qubit RNA BR Assay Kit (Thermo Fisher Scientific). cDNA was generated using the AffinityScript qPCR cDNA Synthesis Kit (Agilent Technologies, Santa Clara, CA, USA) with oligo(dT) primer and stored at −80°C until further use. RT-qPCR was performed with the Brilliant III Ultra-Fast SYBR Green QPCR Master Mix (Agilent Technologies) using the qPCR cycler Mx3000P (Agilent Technologies). Primers were purchased from Qiagen (Hilden, Germany): SDHA (#QT00059486, used as house-keeping gene), CXCR1 (#QT000212919), and CXCR2 (#QT00000518). The relative gene expression was calculated by the $2^{-\Delta\Delta}Ct$ method [45] and results are reported as fold change compared to unstimulated control cells.

Whole Blood Model

The effects of LPS were studied in a human ex vivo whole blood model of a pathogen-associated molecular pattern (PAMP)-driven inflammation as described and validated previously [46]. Following the addition of 0.5 IU/mL heparin (B. Braun Melsungen AG, Melsungen, Germany) and LPS (100 ng/mL) or PBS (control) in native monovettes (Sarstedt, Nürnberg, Germany), 9 mL whole blood was drawn. The specimens were directly transferred under sterile conditions into a system consisting of a Cortiva BioActive Surface (Medtronic, Meerbusch, Germany) coated tubing system. Both ends of the tubes were linked to a circuit using a connector (Medtronic) prepared with the same heparin-based coating technique. This circuit system was mounted on a spinning wheel (Snijders Labs, Tilburg, The Netherlands), rotating at 3 rpm at 37°C. An air bubble inside the system simulated continuous blood circulation. After 1 h, the whole blood was directly transferred into citrate anticoagulated monovettes (Sarstedt) and neutrophils were immediately isolated as described above. In addition, blood gas analysis and complete blood count were performed showing no relevant alterations in pH as well as stable leukocyte, erythrocyte, and platelet count within the incubation period of 1 h (data not shown). To determine CXCR1 (CD181) and CXCR2 (CD182) expression before blood contact with the circuit system and after 1 h with or without 100 ng/mL LPS, whole blood was stained with anti-CD181 PE-Cy7 (BioLegend, San Diego, USA, #320620, final dilution 1:10) and anti-CD182 FITC (BioLegend, #320704, final dilution 1:625), or appropriate isotype controls, for 15 min at 37°C followed by incubation with 1× BD FACS lysing solution™ (BD Biosciences, San Jose, CA, USA) for 30 min at room temperature.

Chemotaxis

To investigate the relationship of ion fluxes and intracellular signaling on IL-8-induced cellular migration, we used a chemotaxis assay in which isolated neutrophils, resuspended in $HBSS^{+/+}$ + 0.1% bovine serum albumin, were incubated with the fluorescent dye 2′,7′-bis-(2-carboxyethyl)-5-(and-6)-carboxyfluorescein (BCECF, 1.6 μg/mL) for 30 min at 37°C. In parallel, neutrophils were incubated with the listed agents: amiloride (200 μM, 10 min, Na^+-channels), UK5099 (400 μM, 30 min, MPC), (4-cyanobenzo[b] thiophene-2-carbonyl)guanidine, methanesulfonate (5 μM, 10 min, NHE1; Calbiochem), W7 (40 μM, 30 min, calmodulin), suramin (200 μM, 30 min, P2Y receptor), calphostin C (50 nM, 30 min, PKC; Cayman Chemicals), 2-deoxyglucose (2 mM, 30 min, glycolysis antimetabolite). Following centrifugation, the neutrophils were resuspended with the corresponding inhibitor in $HBSS^{+/+}$ + 0.1% bovine serum albumin and placed into the upper wells of a 96-well chamber (Neuro Probe, Gaithersburg, MD, USA), separated by a polycarbonate filter with 3 μm pores (Neuro Probe). The chemoattractant IL-8 (or PBS as control) was added to the lower wells of the chamber, which prompted neutrophil migration of the labeled cells in the pores of the membrane. For all experiments, the pharmacological inhibitors were present in both chambers. After 30 min, the increase in BCECF fluorescence was measured in the membrane in order to quantify chemotactic activity. The fluorescence was measured at a wavelength of 485/538 nm using a Fluoroskan Ascent (Thermo Scientific) with the Ascent Software version 2.6.

Data Analysis

Statistical analysis was performed using GraphPad Prism 8 (GraphPad Software Inc., San Diego, USA) and Microsoft Excel (version 16.32). All data are depicted as mean ± SD, when not stated otherwise. Outliers were identified and purged using the z-score. All data were considered to be nonparametric. The significance levels of $p < 0.05$, <0.01, and <0.001 are represented by *, **, and ***, respectively.

Results

IL-8 induced a defined response pattern of neutrophils with significant differences to other inflammatory mediators.

Stimulation of neutrophils with IL-8 (50 ng/mL) resulted in a defined response pattern analyzed by multiparametric flow cytometry as measured after 1, 5, 10, 20, 30, and 60 min. Neutrophils responded with a rapid rise in the FSC (summarized in Fig. 1a, representative donor in online suppl. Fig. 1), with a maximum increase of 107 ± 11% after 10 min. The expansion in cellular size was confirmed by a coulter counter measurement which revealed a rise in diameter from 9.3 ± 0.1 μm under control conditions to 9.6 ± 0.2 μm after 10 min of stimulation with IL-8 ($p < 0.05$, $n = 7$, data not shown). Furthermore, IL-8 induced an increase in pH_i (Fig. 1b), peaking at 5 min (+0.40 ± 0.05, $p < 0.001$ vs. Ctrl). Both effects returned toward the respective control level after 60 min but remained slightly elevated. In addition, neutrophils responded to IL-8 stimulation with depolarization (+3.8 ± 1.6 mV after 1 min, $p < 0.05$ vs. Ctrl, returning to Ctrl levels within 5 min), elevated GlcU (+97 ± 47%, after 10 min $p < 0.001$ vs. Ctrl, Fig. 1c), and an increase in the SSC (+16 ± 3%, after 20 min, $p < 0.001$ vs. Ctrl, Fig. 1c). Stimulating neutrophils with a higher concentration of IL-8 (500 ng/mL) did not result in a further increase in pH_i and FSC (Fig. 1c) but induced a slightly more pronounced depolarization (+5.7 ± 1.6 mV after 1 min, $p < 0.05$ vs. Ctrl, data not shown). No sex-specific differences were observed for all these effects (Fig. 1c). The IL-8 effects on FSC and pH_i were determined to be dose dependent: FSC-EC_{50} 11.5 ng/mL, confidence interval ($CI_{95\%}$): 7.8–16.4 ng/mL (Fig. 1c); pH_i-EC_{50} 9.2 ng/mL, CI: 5.8–14.3 ng/mL (Fig. 1c). The response of neutrophils was similar comparing a faster preparation procedure in the presence of monocytes and leukocytes (online suppl. Table 1).

In the next step, the IL-8-induced response of neutrophils was compared to other inflammatory mediators. All chemoattractants acting through G protein-coupled receptors (IL-8, C5a, and fMLF) evoked a similar response

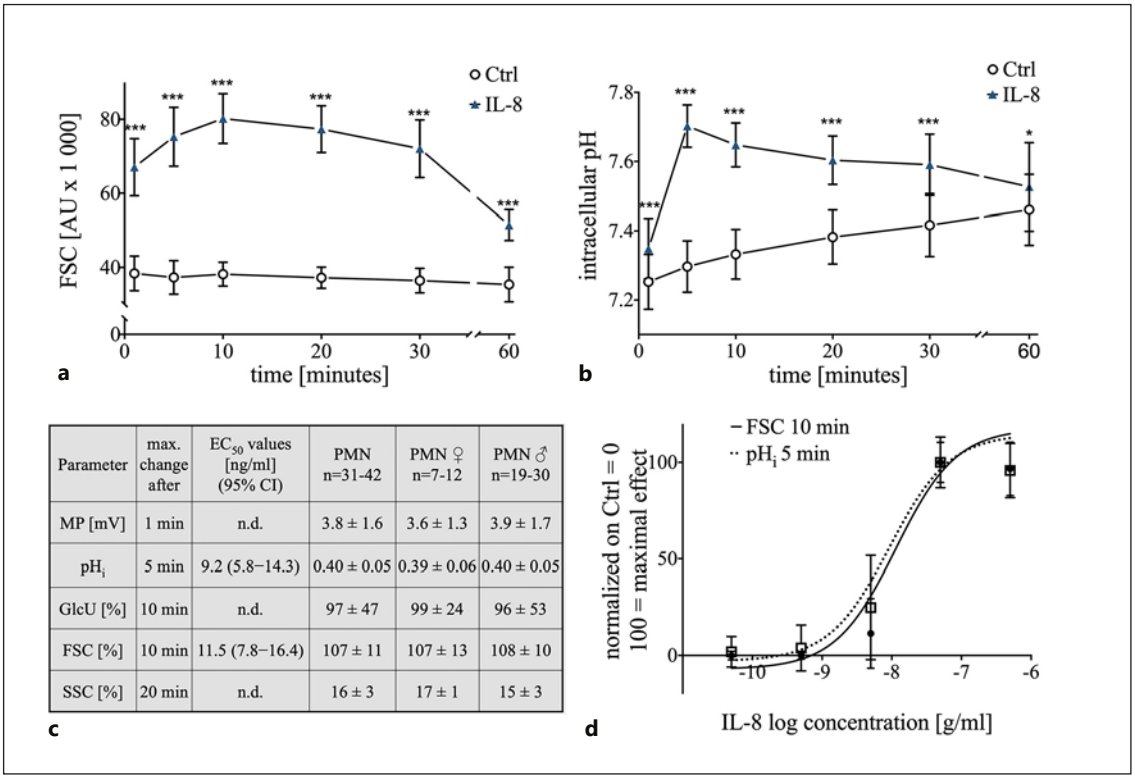

Fig. 1. Concentration dependency and maximal response during the first 60 min of IL-8-induced changes of human neutrophils: **a** Time-dependent effect of the IL-8-induced (50 ng/mL) increase in neutrophil cell shape assessed by FSC; $n = 31–42$; ***, $p < 0.001$ compared to the corresponding Ctrl (Mann-Whitney test). **b** Time course of the IL-8-induced (50 ng/mL) change in pH_i in neutrophils; $n = 31–42$; *, $p < 0.05$; ***, $p < 0.001$ compared to the corresponding Ctrl (Mann-Whitney test). **c** Maximal effect for each measured parameter displayed for all test persons and differentiated by sex and calculated values for EC_{50}. **d** Dose response of the change in cellular shape (FSC) after 10 min and pH_i after 5 min incubation with 0.05–500 ng/mL IL-8; $n = 6–42$. IL, interleukin; pH_i, intracellular pH; FSC, forward scatter area; Ctrl, control; EC_{50}, half-maximal effective concentration; SSC, side scatter area; GlcU, glucose uptake; MP, membrane potential; Ctrl, control; n.d., not determined.

pattern for FSC and pH_i compared to ILs acting through receptors of the immunoglobulin-superfamily (IL-1 and IL-13), type 1 (IL-6), or type 2 (IL-10) cytokine receptors. For LPS as toll-like receptor 4 agonist, no rapid response of neutrophils was detected (Fig. 2 and online suppl. Fig. 2). Compared to fMLF and C5a, IL-8 differed only in its smaller effect on the MP (Fig. 2a, b). IL-8 also induced a minor depolarization but was at the dose applied inferior to C5a and fMLF (Fig. 2c). IL-8, fMLF, and C5a but no other ILs included in this screening evoked an increase in the SSC after 20 min of stimulation (Fig. 2d).

pH_i and Cell Shape Regulation beyond NHE1

The role of several ion channels and transporters on the cellular response after IL-8 stimulation was analyzed with a focus on cellular shape change (FSC) and pH_i. The analyzed proteins and their pharmacological inhibitors were selected based on previous reports on fMLF and C5a [20, 21, 30]. A significant reduction of the IL-8-triggered activity in cellular swelling and intracellular alkalization was obtained by the broad-spectrum inhibition of Na^+-fluxes by amiloride and by the blocking of Cl^--channels by NPPB ($p < 0.05$, Fig. 3a, b). In this context, while a highly selective NHE1 inhibitor did diminish the change of the pH_i ($p < 0.05$, Fig. 3a, b), it did not affect the cellular shape change, indicating the involvement of a NHE1-independent sodium flux that could be inhibited by amiloride (Fig. 3a, b). In contrast, the inhibition of the NBC by S0859 did not inhibit the IL-8-induced response of neutrophils for the cellular shape change and intracellular alkalization (online suppl. Table 1). Furthermore, the blockade of the MPC by UK5099 and of

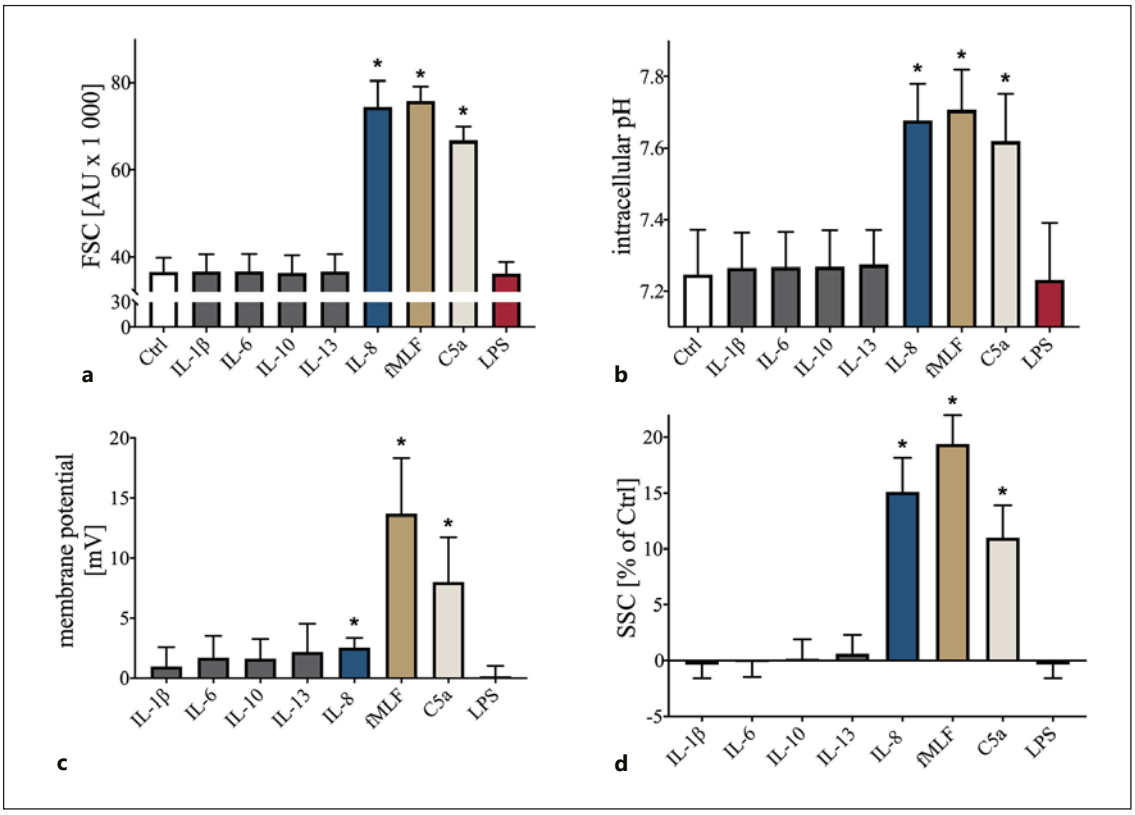

Fig. 2. Comparison of multiple stimuli on the neutrophil cell shape (FSC), pH_i, MP, and granularity (SSC). **a** Influence of various stimuli on the neutrophil cell size after 10 min of incubation with the indicated molecule; n = 6–12; *$p < 0.05$ versus Ctrl (Wilcoxon signed-rank test). **b** Change in pH_i after 5 min of stimulation with the indicated molecule; n = 6–12; *$p < 0.05$ versus Ctrl (Wilcoxon signed-rank test). **c** Effects of numerous stimuli on the resting MP after 1 min of stimulation; n = 6–12; *$p < 0.05$ versus Ctrl (Wilcoxon signed-rank test). **d** Change in neutrophil granularity approximated by the SSC after 20 min of stimulation n = 6–12; *$p < 0.05$ versus Ctrl (Wilcoxon signed-rank test). FSC, forward scatter area; pH_i, intracellular pH; MP, membrane potential; SSC, side scatter area; Ctrl, control; fMLF, N-formyl-Met-Leu-Phe; C5a, complement activation product 5a.

H^+/K^+-ATPase by omeprazole resulted in significant inhibition of the neutrophil response in terms of pH_i and the cell shape following IL-8 stimulation. Inhibition of voltage-gated H^+ channel by zinc resulted in a slight reduction of the cell swelling but did not significantly alter the response in the pH_i (Fig. 3a, b). Inhibition of other transporters and channels that were proposed in previous studies [20, 21, 30] to influence the response of neutrophils but had no significant effects on the IL-8-induced changes are summarized in the online suppl. Table 1.

In addition, intracellular signaling mechanisms were analyzed. By influencing the intracellular calcium levels with SKF-96365 and thapsigargin, IL-8-mediated cell swelling and intracellular alkalization were significantly reduced ($p < 0.05$, Fig. 3a, b). In agreement with this, the blockade of calmodulin with the antimetabolite W7 resulted in a nearly complete abolishment of the IL-8-induced effects ($p < 0.05$ vs. IL-8, Fig. 3a, b). Calphostin C, used as a PKC inhibitor, displayed a minor effect on the change in the FSC but not on the pH_i.

Further comparison of cellular signaling based on the reports for C5a revealed that neutrophils reacted to a blockade of P2Y-purinoceptors by suramin and of aquaporin 9 by copper with a significantly decreased response in cytosolic pH and cellular swelling (Fig. 3a, b). The modulation of HIF-1α by the inductor DMOG revealed a small reduction of the IL-8-induced cell swelling. Inhibition of NADPH oxidase by DPI and blockade of glycolysis with 2-deoxyglucose, the main metabolic pathway, resulted in a significantly reduced cell swelling and intracellular alkalization (Fig. 3a, b).

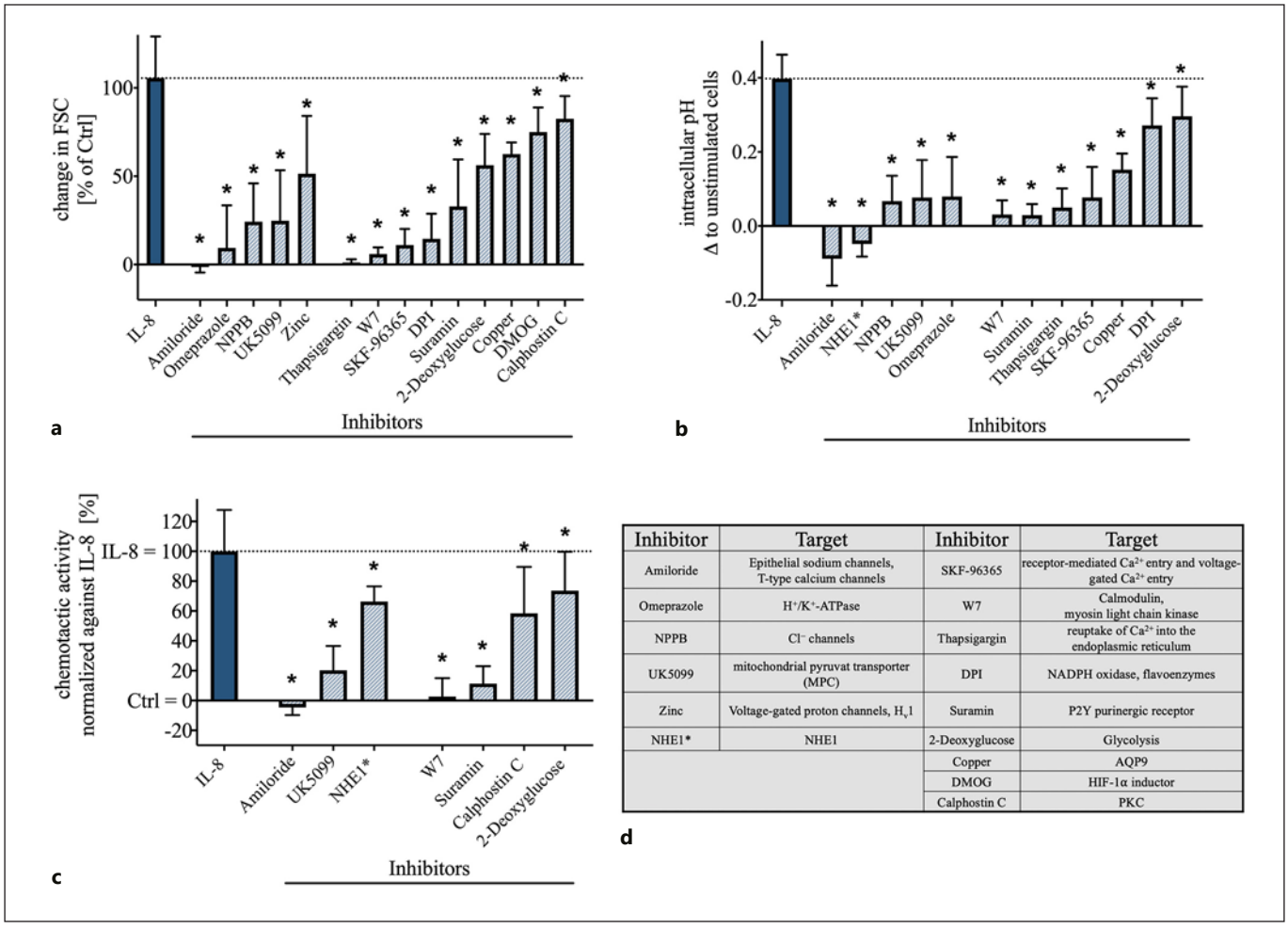

Inhibitor	Target	Inhibitor	Target
Amiloride	Epithelial sodium channels, T-type calcium channels	SKF-96365	receptor-mediated Ca^{2+} entry and voltage-gated Ca^{2+} entry
Omeprazole	H^+/K^+-ATPase	W7	Calmodulin, myosin light chain kinase
NPPB	Cl^- channels	Thapsigargin	reuptake of Ca^{2+} into the endoplasmic reticulum
UK5099	mitochondrial pyruvat transporter (MPC)	DPI	NADPH oxidase, flavoenzymes
Zinc	Voltage-gated proton channels, H_v1	Suramin	P2Y purinergic receptor
NHE1*	NHE1	2-Deoxyglucose	Glycolysis
		Copper	AQP9
		DMOG	HIF-1α inductor
		Calphostin C	PKC

d

Fig. 3. Effect of inhibition of various ion channels and cell signaling molecules on the IL-8-induced change in neutrophil cell shape, intracellular alkalization, and chemotactic activity. **a** Change in IL-8-induced (50 ng/mL) increase in neutrophil cell shape after 5 min modulated by various inhibitors; $n = 5–6$; $^*p < 0.05$ versus IL-8 (Wilcoxon signed-rank test). **b** Influence of the indicated inhibitors on the intracellular alkalization initiated by IL-8 (50 ng/mL) after 5 min; $n = 5–6$; $^*p < 0.05$ versus IL-8 (Wilcoxon signed-rank test). **c** Influence of key inhibitors of IL-8-induced cell swelling and intracellular alkalization on the chemotactic activity, normalized to the activity mediated by IL-8; $n = 6–15$; $^*p < 0.05$ versus IL-8 (Wilcoxon signed-rank test). **d** Summary of the used inhibitors and their suggested target proteins (NHE1* = [4-cyanobenzo[b] thiophene-2-carbonyl]guanidine, methanesulfonate). IL, interleukin; NHE1, sodium proton exchanger 1; FSC, forward scatter area; MPC, mitochondrial pyruvate carrier; H_v1, voltage-gated H^+ channel; PKC, protein kinase C; Ctrl, control.

The chemotactic activity elicited by IL-8, as a central effector function of neutrophils, could be significantly suppressed by blockade of Na^+-channels with amiloride and to a lesser extent by targeting NHE1. Additionally, MPC inhibition (UK5099) reduced IL-8-induced chemotactic activity. Calmodulin (W7), P2Y-purinoreceptors (suramin), PKC (calphostin C), and glucose metabolism (2-deoxyglucose) were also identified as modulators of chemotaxis (Fig. 3c). Figure 3d and online suppl. Table 1 summarize the pharmacological agents and their proposed targets.

PAMP- and Chemotactic Peptides-Mediated Inflammation but Not Acidosis Impaired the Neutrophil Response to IL-8

Severe inflammatory processes are frequently associated with an extracellular acidosis of the microenvironment. After a 10-min incubation in buffers with an altered pH_e, the pH_i value shifted toward the respective externally. Nevertheless, neutrophils still responded independent from the pH_e upon IL-8 with a significant intracellular alkalization ($p < 0.05$ vs. Ctrl of the respective pH_e, Fig. 4a). However, in an alkalotic milieu, IL-

8-stimulated cells revealed a slightly but significantly diminished response in cell shape compared to neutrophils under control conditions (Fig. 4b).

Subsequently, we simulated systemic inflammation by exposure to LPS or various chemoattractants and investigated their influence on the IL-8-induced changes in neutrophil cell shape and pH_i. In vitro exposure to LPS, LPS + LBP, fMLF, or IL-8 for 1 h resulted in an increased FSC and pH_i in comparison with control cells (Fig. 5a, b). The amount of the response was comparable with fMLF- or IL-8-stimulated cells under control conditions. A subsequent stimulation with fMLF or IL-8 caused a significant change in the FSC and pH_i only in nonpretreated cells (Fig. 5a, b). Resting neutrophils or neutrophils under stimulation with IL-8 or fMLF displayed a monomodal distribution for FSC and pH_i. Sole exposure to LPS for 1 h altered FSC and pH_i, but a certain fraction of neutrophils remained unresponsive to these alterations. However, the parallel incubation with LBP reduced and the subsequent stimulation with fMLF or IL-8 completely resolved the fraction of nonresponding neutrophils (Fig. 5a, b). The effects of 1 h of exposure of neutrophils to LPS + LBP on FSC and pH_i reduced the IL-8 mediated change in a dose-dependent manner (FSC: EC_{50} 17.2 ng/mL, $CI_{95\%}$: 7.5–37.2 ng/mL; pH_i: EC_{50} 15.9 ng/mL, CI_{95}%: 5.6–43.6 ng/mL; Fig. 5c–e).

In a translational approach, a clinically relevant human whole blood model was used to confirm the LPS-induced changes ex vivo. Here, exposure to LPS as a relevant stimulus during sepsis displayed similar effects as in vitro. FSC, pH_i, and GlcU were significantly increased after LPS exposure (Fig. 6a–c). Both, in vitro and ex vivo, IL-8 failed to generate a significant response in neutrophils prestimulated with LPS in comparison with control conditions. CXCR1 and CXCR2 level were analyzed to

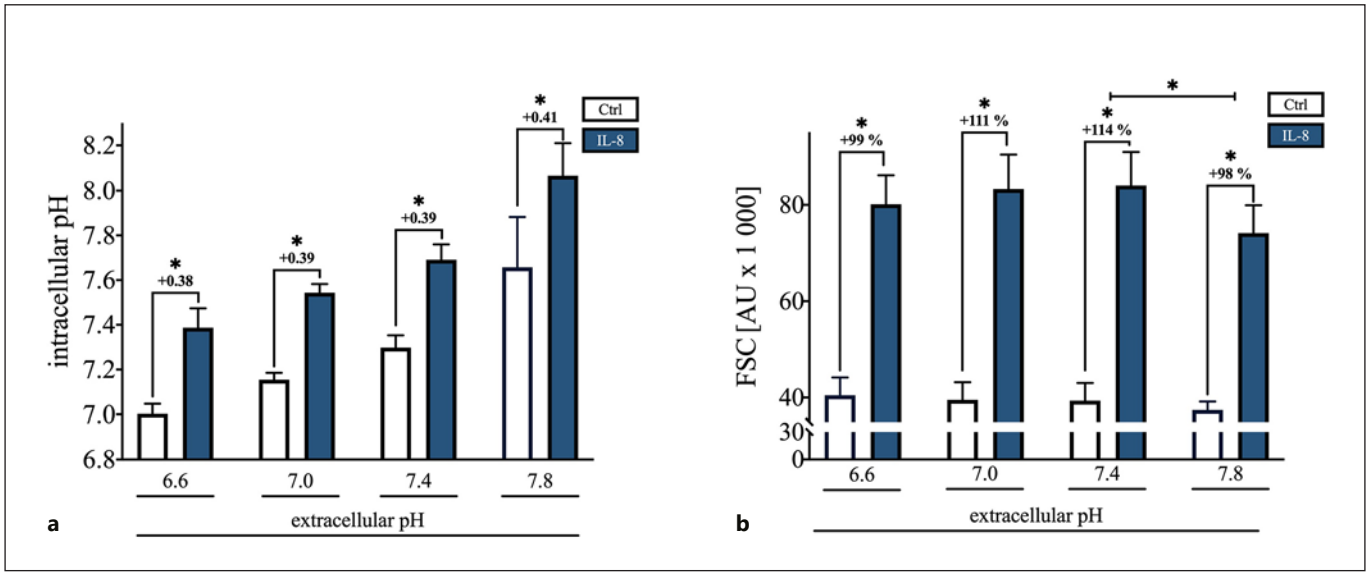

Fig. 4. Influence of a 10-min incubation with various pH_e. **a** Dependency of the pH_i and independency of the IL-8-induced (50 ng/mL) intracellular alkalization from the pH_e; $n = 6$; *$p < 0.05$ versus Ctrl of the related external pH (Mann-Whitney test). **b** Effect of the variation in pH_e on the change in neutrophil cell shape elicited by IL-8 (50 ng/mL); $n = 6$; *$p < 0.05$ FSC of pH_e 7.8 versus IL-8 column with the external pH of 7.4 and FSC of IL-8-stimulated cells with the control of the related external pH (Mann-Whitney test). IL, interleukin; Ctrl, control; pH_e, extracellular pH; pH_i, intracellular pH; FSC, forward scatter area.

Fig. 5. Impact of the preincubation for 1 h with LPS (100 ng/mL), LPS with LBP (2 ng/mL), fMLF (10 μM), and IL-8 (50 ng/mL), on I, F, and $HBSS^{+/+}$ (as Ctrl) induced change in neutrophil cell shape and pH_i. **a** In vitro effect of a preincubation with PAMPs or chemotactic agents on the neutrophil cell shape and on the ability of IL-8 and fMLF to alter the cell size. **b** pH_i after in vitro exposure to the indicated molecules. The data are illustrated as merged violin plots with 2,000 neutrophils from independent donors to report precisely the distribution of the data. Discrepancies between individual donors did not explain the bimodal distribution of FSC and pH_i on exposure to LPS. Preincubation with LPS reduced the IL-8-mediated response in FSC (**c**) and pH_i (**d**). **e** Dose-effect response of the changes in FSC and pH_i after stimulation with 0.1–1,000 ng/mL LPS and 2 ng/mL LBP for 1 h; $n = 5–11$. IL, interleukin; pH_i, intracellular pH; $HBSS^{+/+}$, Hank's Balanced Salt Solution; LBP, LPS-binding protein; PAMP, pathogen-associated molecular pattern; fMLF, N-formyl-Met-Leu-Phe; I, IL-8; F, fMLF; C, $HBSS^{+/+}$; Ctrl, control; FSC, forward scatter area.

(For figure see next page.)

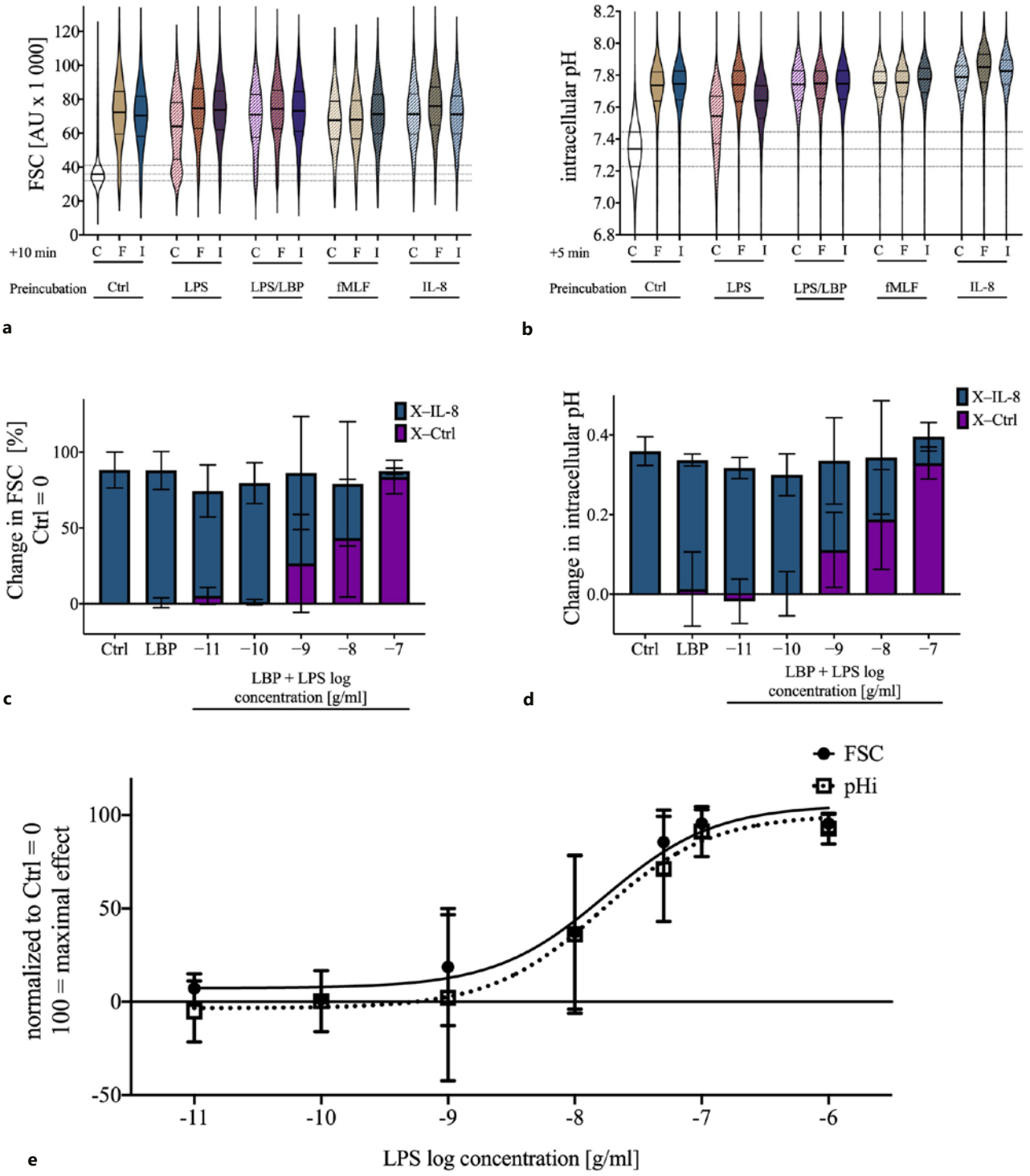
FSC [AU x 1 000]
+10 min
C F I
Preincubation
Ctrl
LPS
LPS/LBP
fMLF
IL-8
a
intracellular pH
+5 min
b
Change in FSC [%] Ctrl = 0
X–IL-8
X–Ctrl
Ctrl
LBP
−11
−10
−9
−8
−7
LBP + LPS log concentration [g/ml]
c
Change in intracellular pH
d
FSC
pHi
normalized to Ctrl = 0
100 = maximal effect
-11
-10
-9
-8
-7
-6
LPS log concentration [g/ml]
e

5

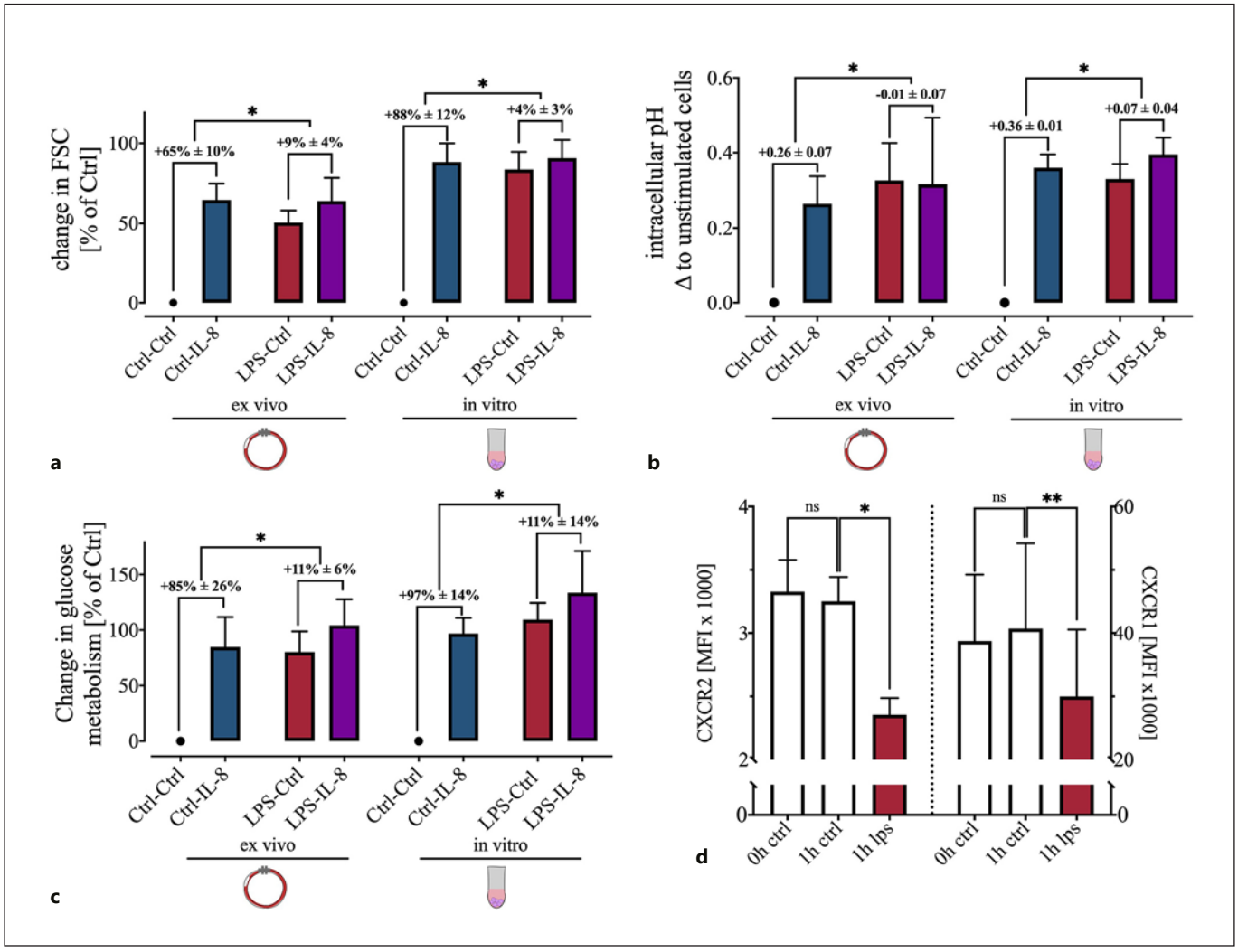

Fig. 6. Comparison of the influence of a 1 h LPS (+LBP for in vitro experiments) preincubation on the IL-8 induced changes in FSC, pH_i, and glucose metabolism between an ex vivo whole blood model and an in vitro model. The delta ± SD between IL-8-stimulated cells and the respective control are shown. **a** LPS caused a significant reduction of the IL-8-induced change in the FSC both in vitro and ex vivo, mainly by raising the control level; $n = 6$; $^*p < 0.05$ (Mann-Whitney test). **b** LPS creates an intracellular alkalization and disrupts the pH shift elicited by IL-8; $n = 6$ $^*p < 0.05$ (Mann-Whitney test). **c** Interaction of LPS with the glucose uptake and reduction of the IL-8-induced increase; $n = 4$–6 $^*p < 0.05$ (Mann-Whitney test). **d** Downregulation of IL-8 receptors CXCR1 (CD181) and CXCR2 (CD182) on the cell surface by LPS treatment for 1 h; $n = 6$; $^*p < 0.05$, $^{**}p < 0.01$ versus Ctrl (one-way ANOVA followed by Dunn's multiple comparisons test). IL, interleukin; pH_i, intracellular pH; LBP, LPS-binding protein; FSC, forward scatter area; Ctrl, control.

exclude a major downregulation of the IL-8 receptors as potential cause of the diminished response. RT-qPCR revealed no alterations in mRNA expression of CXCR1 (fold change 0.8 ± 0.17 compared to unstimulated cells, $p = 0.42$, Mann-Whitney test, $n = 5$) or CXCR2 (fold change 0.99 ± 0.17 compared to unstimulated cells, $p = 0.63$, Mann-Whitney test, $n = 5$). However, LPS induced a significant reduction of the surface expression of both of these receptors after 1 h of stimulation (Fig. 6d).

Every Second Counts to Determine the IL-8-Induced Response Capacity

Finally, a multiparametric continuous flow cytometry measurement of the IL-8-induced alterations was established. Using this near-real-time method, it was clearly shown that there was an initial rapid increase in cell size and pH_i after IL-8 stimulation. Also, the maximal cellular response occurred 2–3 min after stimulation with IL-8. Corresponding values from the same cell isolate prior to

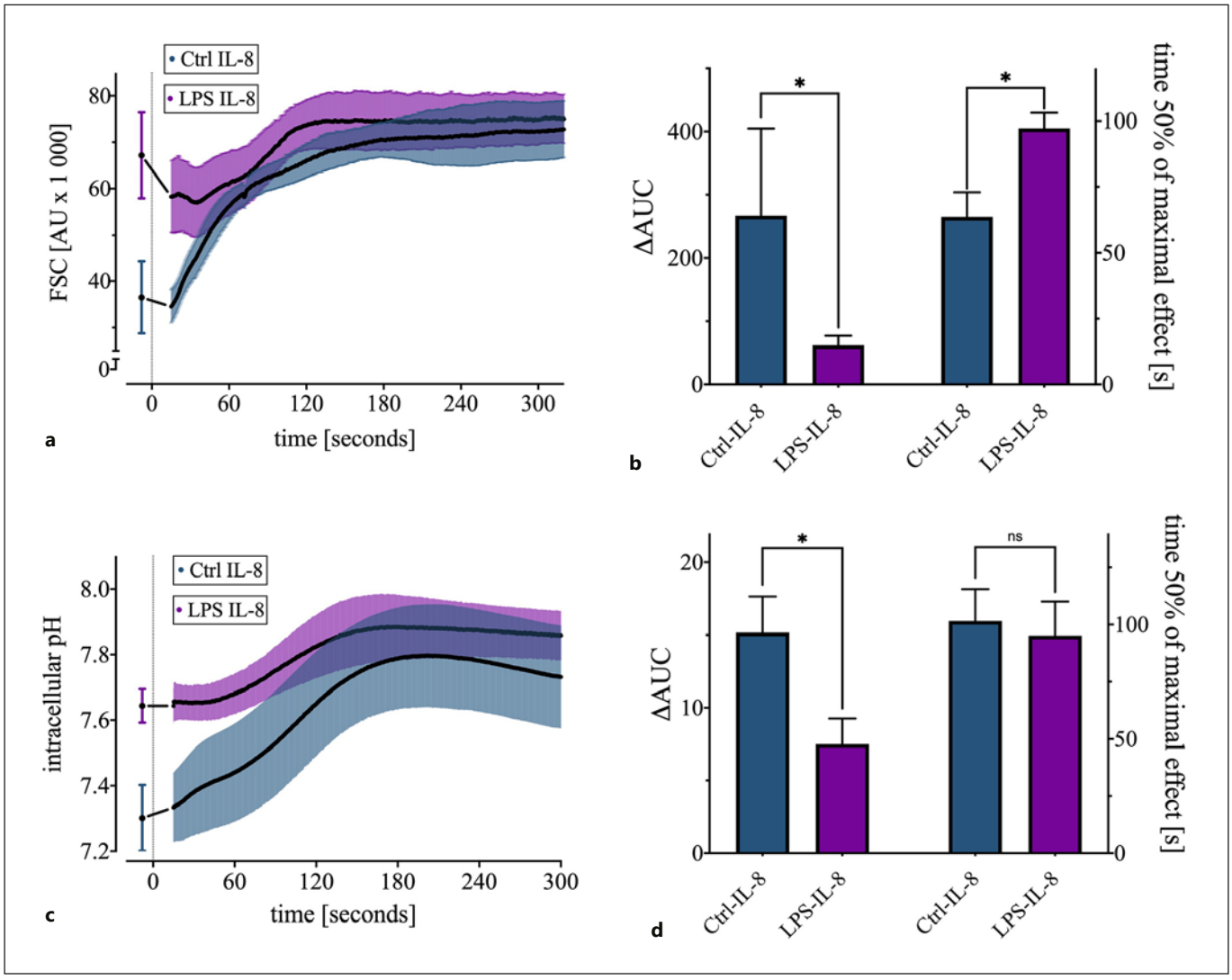

Fig. 7. Near-real-time description of the cellular response to IL-8 with a 1-h exposure to LPS (100 ng/ml) + LBP (2 ng/ml) or PBS as Ctrl. **a** Kinetics of the IL-8-induced reaction in the FSC challenged by LPS; $n = 6$. **b** Effect of LPS pretreatment on the AUC and on the time at which 50% of the maximum cell swelling is attained; $n = 6$, $^*p < 0.05$ (Mann-Whitney test). **c** Influence of LPS on the IL-8-induced alkalization; $n = 6$. **d** Impact of LPS preincubation on the IL-8-induced intracellular alkalization measured by the ΔAUC and the time at which 50% of the maximum alkalization is attained; $n = 6$ $^*p < 0.05$ (Mann-Whitney test). ΔAUC was calculated as the area under the curve subtracted by the rectangular area defined by the initial measurement and zero. LBP, LPS-binding protein, IL, interleukin; FSC, forward scatter area; AUC, area under the curve; Ctrl, control.

treatment served as controls (Fig. 7a, c). When no IL-8 was added, FSC and pH_i remained stable during the measurement process (data not shown). In accordance with the results presented above, LPS pretreatment attenuated the cellular response. The FSC showed that LPS not only influenced the maximum response of neutrophils after IL-8 stimulation but also the time-related kinetics of the IL-8-induced effects. For both parameters, a comparison of the area under the curve (AUC) and the time after which the cells attained 50% of their maximum possible shape change were altered. LPS exposure resulted in less additional swelling of the cells, which was reflected in a significant reduction in the AUC (266 ± 138 without LPS vs. 62 ± 15 with LPS; $p < 0.05$ vs. Ctrl IL-8). Furthermore, LPS significantly prolonged the duration to attaining 50% of the maximum cell swelling (97 ± 6 s with LPS vs. 63 ± 9 s without LPS; $p < 0.05$ vs. Ctrl IL-8; Fig. 7b). Similar results were obtained by analyzing the pH_i. Challenging

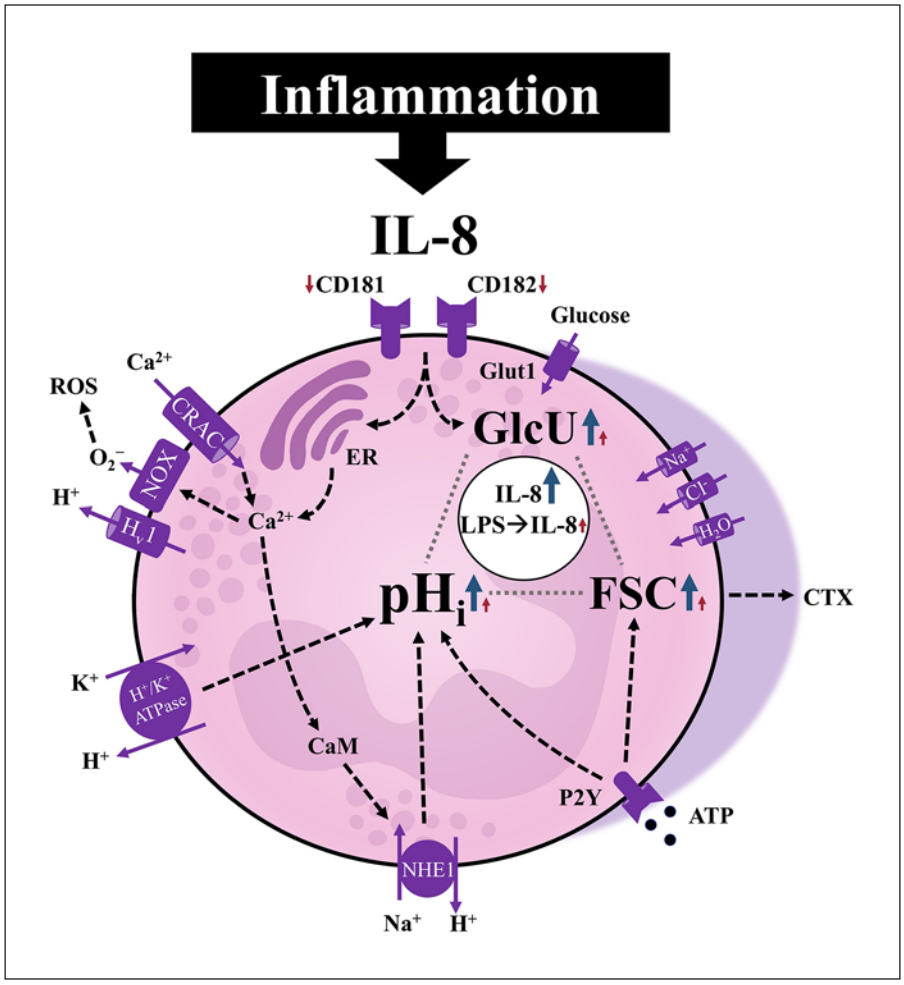

Fig. 8. Graphical summary of the IL-8-induced alterations of neutrophils during health and LPS-mediated inflammation. The IL-8-induced response comprises a significant intracellular alkalization, increased glucose uptake, and change in the cellular shape as indicated by the forward scatter. The transient intracellular alkalization as a major switch of the cellular metabolism was dependent on calcium signaling and the activity of specific ion transporters, predominantly the NHE1. On exposing the neutrophils to LPS in a clinically relevant ex vivo whole blood model system, the cells changed their baseline activity, resulting in a largely diminished additional response that could be triggered by IL-8. Blue/red arrows: IL-8-induced response of neutrophils without/with prior LPS exposure, respectively. IL-8, interleukin 8; CRAC, calcium release-activated channels; ROS, reactive oxygen species; NOX, NADPH oxidase; CaM, calmodulin; NHE1, sodium-proton exchanger 1; pH_i, intracellular pH; FSC, forward scatter area used as indicator for cellular shape change (elongation); GlcU, glucose uptake; CTX, chemotaxis.

the neutrophils with LPS resulted in a significant reduction of the AUC (15 ± 2 without LPS vs. 8 ± 2 with LPS; $p < 0.05$ vs. Ctrl IL-8), as an indication of the diminished ability to alkalinize intracellularly (Fig. 7d).

Discussion

Neutrophils responded to stimulation with IL-8 as summarized in Figure 8. These physiological reactions followed a defined temporal pattern, beginning with peaks in depolarization of the MP after 1 min, intracellular alkalization at 5 min, and maximum cell swelling as well as GlcU after 10 min. For changes in pH_i and cellular shape, a rapid kinetic was demonstrated. The IL-8 concentration used in the present study of 50 ng/mL was higher than the plasma concentration measured in patients with sepsis or in septic shock (mean concentration ± SD: 0.4 ± 0.4, 6.3 ± 9.0 ng/mL, respectively) [47] but comparable to concentrations in pulmonary edema fluid from patients with sepsis (median 84.2 ng/mL) and respiratory distress syndrome [48]. Additionally, the measured EC_{50} values for the cellular activation are in accordance with those previously reported to trigger a maximum calcium influx [49].

The first hallmark of early neutrophil activation, the rapid depolarization of the MP, likely occurs in association with NADPH oxidase activation by the extrusion of electrons [50, 51]. There was a difference in depolarization between the investigated chemotactic peptides. IL-8 induced a significant but lower depolarization in comparison with fMLF and C5a (Fig. 2c). This difference can possibly be explained by the used concentrations [29] that in the present work adhere to clinically relevant values as discussed above.

Multiple other sepsis-relevant inflammatory mediators have been included in this study, such as fMLF (as positive control) and LPS as PAMP representatives and

other ILs, such as IL-6, that is, like IL-8, clinically used as biomarker during sepsis. IL-8 behaved analogously to the inflammatory mediators C5a and fMLF regarding the pH_i but not IL-6 (Fig. 2b). Even lower IL-8 concentrations were capable of triggering pH_i changes, which are involved in the chemotactic response of neutrophils [27–30]. The extrusion of electrons by NADPH oxidase and activation of the hexose monophosphate pathway after stimulation (e.g., by fMLF) results in intracellular acidification and NHE1 transporter activation, which was the proposed underlying mechanism for intracellular alkalization [21, 52–54]. However, to further investigate other ion transporters, including the NBC and AE1, we chose an HCO_3^--containing buffer (RPMI). During the measurement period of 1 h, the control cells became intracellularly more alkaline (Fig. 1b). This can be explained by an increasing alkalization of the RPMI because the buffer requires a CO_2 concentration of 5–10% to maintain its physiological pH. In our experiments, which were repeatedly interrupted by flow cytometric measurements, it was not possible to maintain an absolutely stable CO_2 level, which likely explains the alkalization of the control cells in the measurement process (Fig. 1b). Nevertheless, we used RPMI as a buffer because previous studies demonstrated the clear relevance of bicarbonate in the buffer system and for bicarbonate-dependent transporters, like the AE1, on pH_i and cell shape [36, 55]. Additionally, for fMLF, it has been demonstrated that the presence of HCO_3^- increases the change in pH_i after stimulation [36]. Furthermore, the system was relatively stable during the first 10 min when the maximum intracellular alkalization occurred and it was shown that the IL-8-induced change in pH_i after reaching the maximum was steadily returning to the control level (Fig. 1b).

IL-8 also displayed characteristics similar to C5a and fMLF but not IL-6 in terms of the FSC, a surrogate for the cellular size (Fig. 2a). However, changes in cellular shape, including elongation might also influence this parameter [19]. This hypothesis was supported by the Coulter counter measurements, which indicated a smaller but still significant increase in cellular diameter (+3%) than measured by flow cytometry (+107%). The resulting increase in volume is likely based on a reorganization and polarization of the actin cytoskeleton [20, 32]. Previously published studies suggested that fMLF-induced changes in cell volume and shape are associated with enhanced chemotactic activity [56, 57] and that cellular morphological changes of neutrophils are observable in inflamed tissue [57, 58]. The fMLF concentration used (10 μM) also served as a positive control since this concentration elicits a maximal chemotactic response [59]. It is noteworthy that IL-8 was able to induce similar changes in FSC and pH_i in comparison to C5a (Fig. 2). Overall, this suggests that the IL-8-mediated volume increase is also an important factor for chemotaxis induction and thus a central parameter of neutrophil physiology.

In the context of IL-8-induced stimulation of neutrophils, several studies have indicated the relevance of NHE1 as a regulator of the above mentioned physiological reactions [21, 30] as well as of effector functions, including ROS production [25, 60] and chemotaxis [28]. Our data confirmed an NHE1 dependence of the intracellular alkalization and chemotaxis (Fig. 3b, c). In addition to NHE1, other sodium-dependent effects have also been noted through the inhibition of cellular swelling by amiloride, which are not mediated by NHE1 (Fig. 3a). Therefore, there are NHE1-dependent and -independent sodium effects in the regulation of these physiological reactions as well as IL-8-induced chemotaxis. Moreover, chloride channels, the MPC, and the H^+/K^+-ATPase were involved in FSC and pH_i changes (Fig. 3).

In addition to ion transport proteins, our data indicated, in accordance with previously published results for C5a [21], a regulation of the pH_i through calmodulin and the calcium-signaling pathway (Fig. 3b). There is a strong association of NHE1 activation with the calcium-signaling pathway and calmodulin [61]. Following IL-8 binding to the corresponding receptors CXCR1 and CXCR2, dissociation of the βγ-subunit of the associated G protein with subsequent activation of phospholipase C occurs, which in turn results in mobilization of intracellular calcium and thus activation of calmodulin. In addition to the increase in intracellular calcium, phospholipase C metabolites activate PKC, a central regulator of various neutrophil functions [17, 62]. Compared to C5a, PKC inhibition displayed no effects on the IL-8-initiated alkalization (Fig. 3b) [21]. However, we report a slight influence of PKC on the cell shape change (Fig. 3a). This could be explained by the selectivity of the used blockers because staurosporine inhibits not only PKC but also protein kinase A at similar concentrations [63]. However, the blocker calphostin C applied in this study appears to be more selective for PKC [21, 63]. By contrast, IL-8 and C5a each predominantly use different signaling pathways. For C5a and fMLF, chemotaxis is mediated by the p38/MAPK pathway, whereas IL-8-signaling is dependent on the PI3K/Akt interaction [64]. This appears to be one of the underlying mechanisms for disturbed chemotaxis during severe inflammation because neutrophils preferentially migrate to fMLF, C5a, and LPS [64, 65]. Also, the differ-

ence in signaling could be involved in the varying amount of depolarization comparing IL-8 with fMLF and C5a, besides the dose ranges as mentioned above. In this context, it is also noteworthy that IL-8 and fMLF activate NADPH oxidase differentially [66]. Taken together, because some of the ion transport protein blockers are already approved as drugs, it is tempting to speculate that modulation of the intracellular alkalization might be one strategy to dampen excessive inflammation.

Several earlier studies highlighted the relevance of the IL-8-induced changes during systemic inflammation [19–22]. However, little is known about the interaction of these parameters in an inflammatory environment created by the PAMP LPS. Our data demonstrated that rapid effects within 10 min after LPS stimulation did not induce any significant change in MP, pH_i, or cellular size (Fig. 2a–d, online suppl. 1). By contrast, after a 1 h exposure to LPS, a clear increase in cellular size and an intracellular alkalization were detected (Fig. 5a–d). This effect cannot be explained by IL-8 generation in the whole blood system since exposure to LPS increased the IL-8 level, but far below the EC_{50} (Fig. 1c) of IL-8-induced changes in FSC and pH_i (Ctrl: 46.6 ± 34.6 pg/mL vs. LPS: 160.4 ± 54.5 pg/mL, $n = 10$ as previously published [46]). Surprisingly, after 1 h of LPS stimulation in vitro, the neutrophil population was found to consist of two different groups in terms of cell shape and pH_i (Fig. 5a, b). This effect was diminished in the presence of LBP, highlighting its relevance for LPS sensing by neutrophils. In principle, an alkaline pH_i was already observed in neutrophils of septic patients [21, 67] and mice [21], which could be an LPS-induced effect according to our data. This described heterogeneity of the population is no longer present when the neutrophils are stimulated simultaneously with LBP, suggesting that LBP enhances the LPS response even regarding these physiological parameters [68]. Preincubation with fMLF or IL-8 had a similar suppressive effect as LPS on the IL-8- or fMLF-induced changes in cell shape and pH_i. The apparent difference of changes in FSC and pH_i for 1 h (transiently elevated in Fig. 1, sustained elevated in Fig. 5) exposure of neutrophils to IL-8 is likely explained by the preincubation protocol used in Figure 5, which involved the resuspension of neutrophils after 1 h in buffer including the previously supplemented substance. Previous studies reported that the surface expression of CXCR1 and CXCR2 is reduced after stimulation with LPS involving metalloproteinases and TNF [69, 70], which confirmed the results of the receptor surface expression (Fig. 6d). Interestingly, another study reported downregulation of IL-8 receptor mRNA after 6 h upon LPS stimulation [71]. In addition, LPS exposure of 1 h only slightly diminished IL-8 binding to neutrophils but severely impaired the IL-8-induced chemotactic response [71].

Furthermore, the IL-8-induced effects were also translated in a clinically relevant ex vivo human whole blood model. The data confirmed the results for the FSC and pH_i measured in vitro. In addition, LPS prestimulation led to a higher GlcU (Fig. 6a–c). LPS likely mediates this increased GlcU by a translocation of intracellular vesicular Glut1 transporters to the cell surface [72]. Likewise, for all three of these parameters, IL-8 stimulation after preincubation with LPS induced significantly less marked effects than under control conditions (Fig. 6a–c). We hypothesize that the reduced IL-8-mediated effects of LPS on neutrophils cannot be (fully) explained by a ceiling effect but are an indication that LPS impairs neutrophils in their cellular function; however, this warrants further investigation. It is clear that the cell size physiologically attains a maximum at a certain level. However, regarding the pH_i, the simulation of an in vitro acidosis and alkalosis proved that neutrophils in an alkalotic environment of pH 7.8 can still significantly alter their pH_i (Ctrl [$pH_e = 7.8$] $pH_i = 7.7 \pm 0.23$; IL-8 [$pH_e = 7.8$] $pH_i = 8.1 \pm 0.14$, $p < 0.05$; Fig. 4a). This demonstrates that the neutrophil pH_i could be increased further compared with the LPS-induced alkalization. Anyhow, neutrophils may possibly only generate a certain difference in pH_i and pH_e. In accordance with previous studies [73], we also found an LPS-induced reduction of the detection of surface IL-8 receptors CXCR1/2 as a possible underlying mechanism. In summary, our data suggest that these physiological parameters are significantly altered under inflammatory conditions and the normal response of neutrophils inducible by IL-8 is impaired after LPS exposure. The LPS concentrations required to achieve the half-maximal effects in the FSC and pH_i were significantly higher than the circulating endotoxin concentration in septic patients (Fig. 5c) [74]. However, LPS exposure was only simulated for 1 h, while sepsis patients might be exposed to LPS with lower doses but for a longer period. For the FSC, our data, in agreement with other publications, indicate that these physiological parameters can be used as markers for neutrophils challenged by inflammatory stimuli because not only LPS but also numerous other mediators that occur during severe inflammation induce these alterations [20–22, 29, 30].

To further characterize the IL-8-induced physiological changes as surrogates for the impairment of neutrophils, we investigated the behavior of the cell size and pH_i with a near-real-time flow cytometric measurement method. This up-to-the-second analysis confirmed that LPS expo-

sure not only reduces the maximum IL-8-induced effect but also has an impact on the kinetics of the physiological parameters (Fig. 7a, c). LPS exposure significantly delayed the time until 50% of the maximum effect was attained (Fig. 7b). This measurement method also demonstrated the significantly reduced maximal IL-8-mediated effect by LPS prestimulation. To quantify the IL-8-induced response, we used the increase above the baseline level, defined as the AUC, as a surrogate of the maximum effect (Fig. 7b, d). Similar high temporal resolutions could already be achieved with plate readers [75, 76] but is not yet commonly applied in flow cytometry, which offers the advantage of measuring multiple parameters with a high number of cells, to analyze them separately within the same experiment and thereby to possibly detect subpopulations. As a limitation of these results, it should be noted that although we were able to descriptively show that the above mentioned effects were impaired by LPS, further studies are needed to investigate the underlying molecular mechanisms. Moreover, it needs to be elucidated whether the LPS-mediated changes in the IL-8-induced response are due to a certain kind of preactivation and/or due to a limited possible cellular response range in pH_i and cellular shape.

The presented work has various strengths and limitations. Methodologically, it included a comprehensive analysis of pH_i as a vital function in an appropriate environment containing HCO_3^- and therefore closely resembled plasma regarding the ion concentrations. By inhibiting numerous ion transport proteins and intracellular proteins in an extensive screening approach, the relationship between pH_i, cell swelling, and as an effector function of this, chemotaxis, could be further elucidated. In addition, the present work clearly demonstrated a crucial role for ion transport proteins beyond NHE1 activity in mediating the transient intracellular alkalization evoked by IL-8. The translational relevance of IL-8-induced effects on inflammatory conditions could be investigated on the one hand with a near-real-time measurement and on the other hand in an animal-free human whole blood model. As a limitation, it should be stated that the pH_i was measured indirectly, even though it was performed with a widely used method and was in accordance with the literature [21, 25, 67]. Furthermore, some of the used ion transport protein blockers are not restricted to inhibiting a single channel but also interfere with other proteins. Finally, sepsis was only partially simulated because PAMP exposure and acidosis are only two aspects of this complex disease pattern. Therefore, additional studies should validate these findings in patients with sepsis.

Conclusion

In conclusion, we were able to elucidate the rapid responses of neutrophils to IL-8 stimulation regarding the regulation of cellular shape, pH_i, GlcU, and chemotaxis. Further studies need to determine the possibility to target various ion transport proteins in order to modulate cellular effector functions and to validate these findings in patients with systemic inflammation and sepsis. Additionally, more research is needed to analyze the neutrophil cell shape and pH_i as neutrophil parameters being challenged by LPS and/or IL-8, thereby yielding potential innovative strategies to diagnose and monitor sepsis.

Acknowledgements

The authors are indebted to Ms. Carina Kleimaier, Ms. Anne Rittlinger, and Ms. Bettina Klohs for outstanding technical assistance.

Statement of Ethics

Ethical approval was provided by the Local Independent Ethics Committee of the University of Ulm (number 459/18; 94/14), informed written consent was obtained from healthy human volunteers.

Conflict of Interest Statement

The authors declare that the research was conducted in the absence of any commercial or financial relationship that could be construed as a potential conflict of interest.

Funding Sources

The present work was funded by a research grant ("Forum Gesundheitsstandort") from the Ministry of Science, Research, and Art Baden-Wuerttemberg to D.A.C.M. and M.H.L., a start-up grant, and a "Gerok Rotation" (rotation as clinician scientist) to D.A.C.M. by the Collaborative Research Center 1149 (project number 251293561), German Research Foundation. The funders had no role in the design of this study, data collection or interpretation, or decision to submit results.

Author Contributions

Conceptualization and supervision: D.A.C.M. and M.H.L.; data curation and formal analysis: S.B., S.H., and D.A.C.M.; methodology: S.B., S.H., and D.A.C.M.; validation and visualization: S.B., S.H., C.B., B.T., and D.A.C.M.; writing – original draft: S.B. and D.A.C.M.; and writing – reviewing and editing: all authors.

References

1 Hotchkiss RS, Karl IE. The pathophysiology and treatment of sepsis. N Engl J Med. 2003 Jan 9;348(2):138–50.
2 Kolaczkowska E, Kubes P. Neutrophil recruitment and function in health and inflammation. Nat Rev Immunol. 2013 Mar;13(3):159–75.
3 Baggiolini M, Clark-Lewis I. Interleukin-8, a chemotactic and inflammatory cytokine. FEBS Lett. 1992 Jul 27;307(1):97–101.
4 Alves-Filho JC, de Freitas A, Spiller F, Souto FO, Cunha FQ. The role of neutrophils in severe sepsis. Shock. 2008 Oct;30(Suppl 1):3–9.
5 Shen XF, Cao K, Jiang JP, Guan WX, Du JF. Neutrophil dysregulation during sepsis: an overview and update. J Cell Mol Med. 2017 Sep;21(9):1687–97.
6 Livaditi O, Kotanidou A, Psarra A, Dimopoulou I, Sotiropoulou C, Augustatou K, et al. Neutrophil CD64 expression and serum IL-8: sensitive early markers of severity and outcome in sepsis. Cytokine. 2006 Dec;36(5–6):283–90.
7 Kraft R, Herndon DN, Finnerty CC, Cox RA, Song J, Jeschke MG. Predictive value of IL-8 for sepsis and severe infections after burn injury: a clinical study. Shock. 2015 Mar;43(3):222–7.
8 Schulte W, Bernhagen J, Bucala R. Cytokines in sepsis: potent immunoregulators and potential therapeutic targets: an updated view. Mediators Inflamm. 2013;2013:1–16.
9 Chaudhry H, Zhou J, Zhong Y, Ali MM, McGuire F, Nagarkatti PS, et al. Role of cytokines as a double-edged sword in sepsis. In Vivo. 2013 Dec;27(6):669–84.
10 Harada A, Sekido N, Akahoshi T, Wada T, Mukaida N, Matsushima K. Essential involvement of interleukin-8 (IL-8) in acute inflammation. J Leukoc Biol. 1994;56(5):559–64.
11 Huber AR, Kunkel SL, Todd RF, Weiss SJ. Regulation of transendothelial neutrophil migration by endogenous interleukin-8. Science. 1991 Oct 4;254(5028):99–102.
12 Detmers PA, Lo SK, Olsen-Egbert E, Walz A, Baggiolini M, Cohn ZA. Neutrophil-activating protein 1/interleukin 8 stimulates the binding activity of the leukocyte adhesion receptor CD11b/CD18 on human neutrophils. J Exp Med. 1990 Apr 1;171(4):1155–62.
13 Bréchard S, Bueb JL, Tschirhart EJ. Interleukin-8 primes oxidative burst in neutrophil-like HL-60 through changes in cytosolic calcium. Cell Calcium. 2005 Jun;37(6):531–40.
14 Henkels KM, Frondorf K, Gonzalez-Mejia ME, Doseff AL, Gomez-Cambronero J. IL-8-induced neutrophil chemotaxis is mediated by Janus kinase 3 (JAK3). FEBS Lett. 2011 Jan 3;585(1):159–66.
15 Cummings CJ, Martin TR, Frevert CW, Quan JM, Wong VA, Mongovin SM, et al. Expression and function of the chemokine receptors CXCR1 and CXCR2 in sepsis. J Immunol. 1999 Feb 15;162(4):2341–6.
16 Raghuwanshi SK, Su Y, Singh V, Haynes K, Richmond A, Richardson RM. The chemokine receptors CXCR1 and CXCR2 couple to distinct G protein-coupled receptor kinases to mediate and regulate leukocyte functions. J Immunol. 2012 Sep 15;189(6):2824–32.
17 Ha H, Debnath B, Neamati N. Role of the CXCL8-CXCR1/2 axis in cancer and inflammatory diseases. Theranostics. 2017;7(6):1543–88.
18 Gennaro R, Pozzan T, Romeo D. Monitoring of cytosolic free Ca2+ in C5a-stimulated neutrophils: loss of receptor-modulated Ca2+ stores and Ca2+ uptake in granule-free cytoplasts. Proc Natl Acad Sci U S A. 1984 Mar 1;81(5):1416–20.
19 Messerer DAC, Denk S, Föhr KJ, Halbgebauer R, Braun CK, Hönes F, et al. Complement C5a alters the membrane potential of neutrophils during hemorrhagic shock [Internet]. Mediators Inflamm. 2018 [cited 2019 May 20]. Available from: https://www.hindawi.com/journals/mi/2018/2052356/.
20 Denk S, Taylor RP, Wiegner R, Cook EM, Lindorfer MA, Pfeiffer K, et al. Complement C5a-induced changes in neutrophil morphology during inflammation. Scand J Immunol. 2017 Sep;86(3):143–55.
21 Denk S, Neher MD, Messerer DAC, Wiegner R, Nilsson B, Rittirsch D, et al. Complement C5a functions as a master switch for the pH balance in neutrophils exerting fundamental immunometabolic effects. J Immunol. 2017 Jun 15;198(12):4846–54.
22 Hesselink L, Heeres M, Paraschiakos F, ten Berg M, Huisman A, Hoefer IE, et al. A rise in neutrophil cell size precedes organ dysfunction after trauma. Shock. 2019 Apr;51(4):439–46.
23 Department of Laboratories, University of the Philippines-Philippine General Hospital, Villanueva EI, Almirol BJ, Department of Epidemiology and Biostatistics, University of the Philippines-College of Public Health. The accuracy of mean neutrophil volume relative to blood culture for the diagnosis of sepsis: a meta-analysis. PJP. 2017 Apr 26;2(1):18–22.
24 Wu D, Kraut JA. Potential role of NHE1 (sodium-hydrogen exchanger 1) in the cellular dysfunction of lactic acidosis: implications for treatment. Am J Kidney Dis. 2011 May;57(5):781–7.
25 Coakley RJ, Taggart C, McElvaney NG, O'Neill SJ. Cytosolic pH and the inflammatory microenvironment modulate cell death in human neutrophils after phagocytosis. Blood. 2002 Nov 1;100(9):3383–91.
26 Grinstein S, Swallow CJ, Rotstein OD. Regulation of cytoplasmic pH in phagocytic cell function and dysfunction. Clin Biochem. 1991 Jun;24(3):241–7.
27 Hayashi H, Aharonovitz O, Alexander RT, Touret N, Furuya W, Orlowski J, et al. Na+/H+ exchange and pH regulation in the control of neutrophil chemokinesis and chemotaxis. Am J Physiol Cell Physiol. 2008 Feb;294(2):C526–34.
28 Simchowitz L, Cragoe EJ. Regulation of human neutrophil chemotaxis by intracellular pH. J Biol Chem. 1986 May 15;261(14):6492–500.
29 Yuo A, Kitagawa S, Kasahara T, Matsushima K, Saito M, Takaku F. Stimulation and priming of human neutrophils by interleukin-8: cooperation with tumor necrosis factor and colony-stimulating factors. Blood. 1991 Nov 15;78(10):2708–14.
30 Ritter M, Schratzberger P, Rossmann H, Wöll E, Seiler K, Seidler U, et al. Effect of inhibitors of Na+/H+-exchange and gastric H+/K+ ATPase on cell volume, intracellular pH and migration of human polymorphonuclear leucocytes. Br J Pharmacol. 1998 Jun;124(4):627–38.
31 O'Flaherty JT, Kreutzer DL, Ward PA. Neutrophil aggregation and swelling induced by chemotactic agents. J Immunol. 1977 Jul;119(1):232–9.
32 Lepidi H, Zaffran Y, Ansaldi JL, Mege JL, Capo C. Morphological polarization of human polymorphonuclear leucocytes in response to three different chemoattractants: an effector response independent of calcium rise and tyrosine kinases. J Cell Sci. 1995 Apr;108(Pt 4):1771–8.
33 Simchowitz L, Roos A. Regulation of intracellular pH in human neutrophils. J Gen Physiol. 1985 Mar;85(3):443–70.
34 Maueröder C, Mahajan A, Paulus S, Gößwein S, Hahn J, Kienhöfer D, et al. Ménage-à-trois: the ratio of bicarbonate to CO2 and the pH regulate the capacity of neutrophils to form NETs. Front Immunol [Internet]. 2016 Dec 9. [cited 2020 May 6];7. Available from: http://journal.frontiersin.org/article/10.3389/fimmu.2016.00583/full.
35 Giambelluca MS, Ciancio MC, Orlowski A, Gende OA, Pouliot M, Aiello EA. Characterization of the Na/HCO3− cotransport in human neutrophils. Cell Physiol Biochem. 2014;33(4):982–90.
36 Giambelluca MS, Gende OA. Cl^-/HCO_3^- exchange activity in fMLP-stimulated human neutrophils. Biochem Biophys Res Commun. 2011 Jun;409(3):567–71.
37 Nie M, Yang L, Bi X, Wang Y, Sun P, Yang H, et al. Neutrophil extracellular traps induced by IL8 promote diffuse large B-cell lymphoma progression via the TLR9 signaling. Clin Cancer Res. 2019 Mar 15;25(6):1867–79.
38 Wang M, Zhong D, Dong P, Song Y. Blocking CXCR1/2 contributes to amelioration of lipopolysaccharide-induced sepsis by downregulating substance P. J Cell Biochem. 2019 Feb;120(2):2007–14.

39 Leitner JM, Mayr FB, Firbas C, Spiel AO, Steinlechner B, Novellini R, et al. Reparixin, a specific interleukin-8 inhibitor, has no effects on inflammation during endotoxemia. Int J Immunopathol Pharmacol. 2007 Jan;20(1):25–36.
40 Zarbock A, Allegretti M, Ley K. Therapeutic inhibition of CXCR2 by Reparixin attenuates acute lung injury in mice: CXCR2 inhibitor protects against ALI. Br J Pharmacol. 2009 Jan 29;155(3):357–64.
41 Deventer SJH, Möhlen MAM, Poll T. Potential importance of IL-8: a potent chemokine, in sepsis. In: Vincent JL, editor. Yearbook of intensive care and emergency medicine 1993 [Internet]. Berlin, Heidelberg: Springer; 1993. p. 114–21 [cited 2020 Jun 3]. Available from: http: //link.springer.com/10.1007/978-3-642-84904-6_11.
42 Mera S, Tatulescu D, Cismaru C, Bondor C, Slavcovici A, Zanc V, et al. Multiplex cytokine profiling in patients with sepsis: simultaneous analysis of 17 cytokines in sepsis. APMIS. 2011 Feb;119(2):155–63.
43 Dhingra N. Safe Injection Global Network, World Health Organization. WHO guidelines on drawing blood: best practices in phlebotomy [Internet]. 2010 [cited 2020 Aug 25]. Available from: http://www.ncbi.nlm.nih.gov/books/NBK138650/.
44 Denk S. Complement C5a-induzierte Funktionsänderung neutrophiler Granulozyten während der systemischen Entzündung. Universität Ulm; 2017.
45 Schmittgen TD, Livak KJ. Analyzing real-time PCR data by the comparative C(T) method. Nat Protoc. 2008 Jun;3(6):1101–8.
46 Messerer DAC, Vidoni L, Erber M, Stratmann AEP, Bauer JM, Braun CK, et al. Animal-free human whole blood sepsis model to study changes in innate immunity. Front Immunol. 2020;11:571992.
47 Endo S, Inada K, Ceska M, Takakuwa T, Yamada Y, Nakae H, et al. Plasma interleukin 8 and polymorphonuclear leukocyte elastase concentrations in patients with septic shock. J Inflamm. 1995;45(2):136–42.
48 Miller EJ, Cohen AB, Matthay MA. Increased interleukin-8 concentrations in the pulmonary edema fluid of patients with acute respiratory distress syndrome from sepsis. Crit Care Med. 1996 Sep;24(9):1448–54.
49 Rose JJ, Foley JF, Murphy PM, Venkatesan S. On the mechanism and significance of ligand-induced internalization of human neutrophil chemokine receptors CXCR1 and CXCR2. J Biol Chem. 2004 Jun 4;279(23):24372–86.
50 Jankowski A, Grinstein S. A noninvasive fluorimetric procedure for measurement of membrane potential: quantification of the NADPH oxidase-induced depolarization in activated neutrophils. J Biol Chem. 1999 Sep 10; 274(37):26098–104.
51 DeCoursey TE. Interactions between NADPH oxidase and voltage-gated proton channels: why electron transport depends on proton transport. FEBS Lett. 2003 Nov 27;555(1):57–61.
52 Borregaard N, Schwartz JH, Tauber AI. Proton secretion by stimulated neutrophils. Significance of hexose monophosphate shunt activity as source of electrons and protons for the respiratory burst. J Clin Invest. 1984 Aug; 74(2):455–9.
53 Nanda A, Grinstein S, Curnutte JT. Abnormal activation of H+ conductance in NADPH oxidase-defective neutrophils. Proc Natl Acad Sci U S A. 1993 Jan 15;90(2):760–4.
54 Nanda A, Gukovskaya A, Tseng J, Grinstein S. Activation of vacuolar-type proton pumps by protein kinase C. Role in neutrophil pH regulation. J Biol Chem. 1992 Nov 15;267(32): 22740–6.
55 Simchowitz L, Textor JA, Vogt SK. Use of tributyltin to probe contribution of Cl(-)-HCO3- exchange to regulation of steady-state pHi in human neutrophils. Am J Physiol. 1991 Nov 1;261(5 Pt 1):C906–15.
56 Simchowitz L, Cragoe EJ. Inhibition of chemotactic factor-activated Na+/H+ exchange in human neutrophils by analogues of amiloride: structure-activity relationships in the amiloride series. Mol Pharmacol. 1986 Aug;30(2):112–20.
57 Rosengren S, Henson PM, Worthen GS. Migration-associated volume changes in neutrophils facilitate the migratory process in vitro. Am J Physiol. 1994 Dec 1;267(6 Pt 1):C1623–32.
58 Worthen GS, Henson PM, Rosengren S, Downey GP, Hyde DM. Neutrophils increase volume during migration in vivo and in vitro. Am J Respir Cell Mol Biol. 1994 Jan 1;10(1): 1–7.
59 Huber-Lang M, Sarma VJ, Lu KT, McGuire SR, Padgaonkar VA, Guo RF, et al. Role of C5a in multiorgan failure during sepsis. J Immunol. 2001 Jan 15;166(2):1193–9.
60 Behnen M, Möller S, Brozek A, Klinger M, Laskay T. Extracellular acidification inhibits the ROS-dependent formation of neutrophil extracellular traps. 2017 Feb 28 [cited 2019 Apr 23];8. Available from: https://www.ncbi.nlm.nih.gov/pmc/articles/PMC5329032/.Front Immunol [Internet]
61 Bertrand B, Wakabayashi S, Ikeda T, Pouysségur J, Shigekawa M. The Na+/H+ exchanger isoform 1 (NHE1) is a novel member of the calmodulin-binding proteins. Identification and characterization of calmodulin-binding sites. J Biol Chem. 1994 May 6;269(18): 13703–9.
62 Bertram A, Ley K. Protein kinase C isoforms in neutrophil adhesion and activation. Arch Immunol Ther Exp. 2011 Apr;59(2):79–87.
63 Tamaoki T. Use and specificity of staurosporine, UCN-O1, and calphostin C as protein kinase inhibitors. In: Methods in enzymology [internet]. Elsevier; 1991. p. 340–7 [cited 2020 Jun 16]. Available from: https://linkinghub.elsevier.com/retrieve/pii/0076687991010306.
64 Heit B, Tavener S, Raharjo E, Kubes P. An intracellular signaling hierarchy determines direction of migration in opposing chemotactic gradients. J Cell Biol. 2002 Oct 14;159(1):91–102.
65 Wang X, Qin W, Zhang Y, Zhang H, Sun B. Endotoxin promotes neutrophil hierarchical chemotaxis via the p38-membrane receptor pathway. Oncotarget. 2016 Nov 8;7(45): 74247–58.
66 Fu H, Bylund J, Karlsson A, Pellmé S, Dahlgren C. The mechanism for activation of the neutrophil NADPH-oxidase by the peptides formyl-Met-Leu-Phe and Trp-Lys-Tyr-Met-Val-Met differs from that for interleukin-8. Immunology. 2004 Jun;112(2):201–10.
67 Sachse C, Wolterink G, Pallua N. Neutrophil intracellular pH and phagocytosis after thermal trauma. Clin Chim Acta. 2000 May 1; 295(1–2):13–26.
68 Yan SR, Al-Hertani W, Byers D, Bortolussi R. Lipopolysaccharide-binding protein- and CD14-dependent activation of mitogen-activated protein kinase p38 by lipopolysaccharide in human neutrophils is associated with priming of respiratory burst. Infect Immun. 2002 Aug;70(8):4068–74.
69 Khandaker MH, Mitchell G, Xu L, Andrews JD, Singh R, Leung H, et al. Metalloproteinases are involved in lipopolysaccharide- and tumor necrosis factor-alpha-mediated regulation of CXCR1 and CXCR2 chemokine receptor expression. Blood. 1999 Apr 1;93(7): 2173–85.
70 Tikhonov I, Doroshenko T, Chaly Y, Smolnikova V, Pauza CD, Voitenok N. Down-regulation of CXCR1 and CXCR2 expression on human neutrophils upon activation of whole blood by S. aureus is mediated by TNF-alpha. Clin Exp Immunol. 2001 Sep;125(3):414–22.
71 Biragyn A. Granulocyte-colony stimulating factor and lipopolysaccharide regulate the expression of interleukin 8 receptors on polymorphonuclear leukocytes. J Biol Chem. 1995 Nov 24;270(47):28188–92.
72 Schuster DP, Brody SL, Zhou Z, Bernstein M, Arch R, Link D, et al. Regulation of lipopolysaccharide-induced increases in neutrophil glucose uptake. Am J Physiol Lung Cell Mol Physiol. 2007 Apr 1;292(4):L845–51.
73 Sabroe I, Jones EC, Whyte MK, Dower SK. Regulation of human neutrophil chemokine receptor expression and function by activation of toll-like receptors 2 and 4. Immunology. 2005 May;115(1):90–8.
74 Opal SM, Scannon PJ, Vincent J, White M, Carroll SF, Palardy JE, et al. Relationship between plasma levels of lipopolysaccharide (LPS) and LPS-binding protein in patients with severe sepsis and septic shock. J Infect Dis. 1999 Nov;180(5):1584–9.
75 Monteith G, Bird G. Techniques: high-throughput measurement of intracellular Ca: back to basics. Trends Pharmacol Sci. 2005 Apr;26(4):218–23.
76 Schaff UY, Yamayoshi I, Tse T, Griffin D, Kibathi L, Simon SI. Calcium flux in neutrophils synchronizes beta2 integrin adhesive and signaling events that guide inflammatory recruitment. Ann Biomed Eng. 2008 Apr;36(4): 632–46.